

Communication

Glyphosate Removal from Water Using Biochar Based Coffee Husk Loaded Fe₃O₄

Arestha Leo Lita ^{1,2}, Ender Hidayat ^{3,4,*}, Nur Maisarah Mohamad Sarbani ^{3,4}, Hiroyuki Harada ^{3,4},
Seiichiro Yonemura ^{3,4}, Yoshiharu Mitoma ^{3,4}, Herviyanti ² and Gusmini ²

¹ Exchange Student Program, Faculty of Bioresources Science, Prefectural University of Hiroshima, Shobara 727-0023, Japan

² Department of Soil Science and Land Resource, Faculty of Agriculture, Andalas University, Limau Manis, Padang City 25164, Indonesia

³ Graduate School of Comprehensive and Scientific Research, Prefectural University of Hiroshima, Shobara 727-0023, Japan

⁴ Department of Life Science, Faculty of Bioresources Science, Prefectural University of Hiroshima, Shobara 727-0023, Japan

* Correspondence: hidayatendar1@gmail.com

Abstract: Glyphosate is an herbicide that is usually used by farmers and is considered harmful to the environment in excess amounts. To address these issues, coffee-husk-biochar-loaded Fe₃O₄ (CHB-Fe₃O₄) was used as an adsorbent to remove glyphosate from water. CHB-Fe₃O₄ characteristics such as p*H*_{pzc}, FTIR, and SEM were measured to understand the properties of this adsorbent. The best conditions for glyphosate removal by CHB-Fe₃O₄ were obtained at pH 2.0, where the adsorption capacity and percentage removal are 22.44 mg/g and 99.64%, respectively, after 4 h of adsorption. The Freundlich model provided the best fit for the adsorption isotherm, demonstrating multilayer sorption. The most effective model for characterizing the adsorption kinetics was the pseudo-second-order model with a chemical adsorption mechanism. The desorption studies found that the use of 0.1 M NaOH was the best concentration to effectively desorb glyphosate with a desorption percentage of 69.4%. This indicates that CHB-Fe₃O₄ is a feasible adsorbent for glyphosate removal from water.

Keywords: adsorption; desorption; glyphosate; isotherm; coffee husk biochar; kinetics



Citation: Lita, A.L.; Hidayat, E.; Mohamad Sarbani, N.M.; Harada, H.; Yonemura, S.; Mitoma, Y.; Herviyanti, Gusmini. Glyphosate Removal from Water Using Biochar Based Coffee Husk Loaded Fe₃O₄. *Water* **2023**, *15*, 2945. <https://doi.org/10.3390/w15162945>

Academic Editors: Natalija Velić, Marija Stjepanović and Nataša Jović-Jovičić

Received: 30 June 2023

Revised: 8 August 2023

Accepted: 14 August 2023

Published: 15 August 2023



Copyright: © 2023 by the authors. Licensee MDPI, Basel, Switzerland. This article is an open access article distributed under the terms and conditions of the Creative Commons Attribution (CC BY) license (<https://creativecommons.org/licenses/by/4.0/>).

1. Introduction

Glyphosate (C₃H₈NO₅P), also known as N-phosphonmethyl glycine, is one of the active ingredients in herbicides that is commonly used by farmers to eradicate postharvest weeds. In the last few years, glyphosate usage has increased annually, by about 8.6 million kilograms from 1974 to 2014 [1]. The uncontrolled application of herbicides containing this active ingredient (glyphosate) without adhering to the recommended levels can cause serious damage to environmental ecosystems, especially soil and water. Glyphosate enters the water system through several sources such as agricultural runoff from rainfall or irrigation and groundwater leakage from contaminated crop residues [2]. The current detection of glyphosate, and its transforming products amino methyl phosphonic acid, in food, human bodily fluids, waterways, and soil demonstrates an urgent need for further research on how this herbicide affects the environment [3]. The usage of glyphosate exceeding the threshold level can have adverse effects on the environment, human health, and aquatic organisms, and can also impart ecological threats to sustainable agriculture [4]. This herbicide can penetrate into water systems and threaten and cause damage to ecosystems as it generally remains in the environment for a long time and is carcinogenic. The presence of herbicides in drinking water can cause major health problems to humans, therefore it is necessary to monitor the concentration of this herbicide in tap water [5]. A previous study has reported that tap water and river water have the slowest degradation rate of glyphosate. This is

because the organic carbon content contained in these waters absorbed most of the photons, therefore slowing down the degradation rate of the herbicide [6]. Thus, an effective solution is needed to treat glyphosate-contaminated wastewaters and streams to prevent excess concentration of this toxin and to avoid the glyphosate from interfering with the human food chain [5].

Glyphosate contamination in the environment has driven scientists to develop efficient and reliable methods to purify water resources. As highlighted by previous researchers, the urgent need to remove this substance has led to the development of various appropriate and practical alternatives [7–11]. There are many conventional methods that have been conducted by several researchers to remove contaminants from water, such as membrane separation [12], microwave UV [13], UV irradiation [14], biodegradation [15], and the most popular method of adsorption [16,17]. Adsorption is frequently preferred as the alternative removal method for various reasons, including the fact that the process may be personalized to specific applications (selectable for dissolved glyphosate), and the adsorbent material is considered to be relatively safe to handle [18,19].

There are various types of adsorbents that have been synthesized for glyphosate adsorption, such as magnetic-coated silica trimethyl chitosan hybrid shells [20], zinc oxide nanoparticles [21], Mg-Al-layered double oxides [22], and clay biochar [23]. However, certain aspects, such as accessibility of the adsorbent's materials and the abundant waste produced from agricultural industries, including coffee husks, need to be considered in order to fully utilize the source and minimize the waste. In 2021–2022, coffee husk production reached 0.3 billion tons [24], and this waste is discarded near the factory, which can pollute the environment [25]. Therefore, instead of discarding the coffee husk to the environment, this research intends to utilize it as an effective adsorbent material.

In conjunction with this issue, coffee husks that undergo heat treatment to produce biochar (a pyrolysis process of numerous types of biomasses under low-concentrated oxygen conditions) have been proven to hold great potential to create adsorbent material [26]. Several studies have used coffee husk biochar to remove pollutants, such as dye and heavy metals [27,28]. However, there is no reported study on the use of magnetite coffee husk biochar to remove glyphosate from water. In this study, we synthesized coffee husk biochar with magnetite properties to remove glyphosate. The raw coffee husk was burned at 600 °C for 2 h. Subsequently, Fe₃O₄ is coated to the biochar to increase the number of surface-active sites. The adsorption process and mechanism of CHB-Fe₃O₄ adsorbing glyphosate were investigated by analyzing its isotherm and through kinetic studies.

2. Materials and Methods

2.1. Materials and Chemicals

Glyphosate with purity of 95% was purchased from Anhui Fengle Agrochemical Co, Ltd. Hefei, China. Sodium oxide (NaOH), sodium chloride (NaCl), and sodium molybdate (Na₂MoO₄) were bought from Kanto Chemical CO., INC, Tokyo, Japan. Ninhydrin (C₉H₆O₄) was obtained from Sigma Aldrich chemicals, MA, USA.

2.2. Preparation of Coffee Husk Biochar (CHB)

Coffee husk was obtained from Solok Radjo Cooperative, West Sumatera province, Indonesia. Coffee husk (CH) was ground and sieved into a fine particle size < 2 mm, and then burned using a Muffle furnace (FO100, Yamato, Japan) at temperature 600 °C for 2 h with a heating rate of 10 °C min⁻¹ under nitrogen atmosphere (Figure 1). The coffee husk biochar (CHB) was then stored in a desiccator before further treatment.

2.3. Preparation of Coffee-Husk-Biochar-Loaded Fe₃O₄ (CHB-Fe₃O₄)

CHB (3 g) was mixed with FeSO₄·7H₂O (0.5 M) and FeCl₃ (1 M). Then, the mixed solution was shaken for 1 h while heated at 60 °C. Then, the mixture was stirred for 24 h at 25–30 °C by using a magnetic stirrer (Mag-mixer MG600) after adjusting the pH to 10 by using 3 M NaOH. Following that, the filtration process by filtering the mixture using filter

paper (qualitative filter paper no. 5C) was performed, and the filtrate was dried for 72 h at 60 °C. This adsorbent is called CHB-Fe₃O₄.

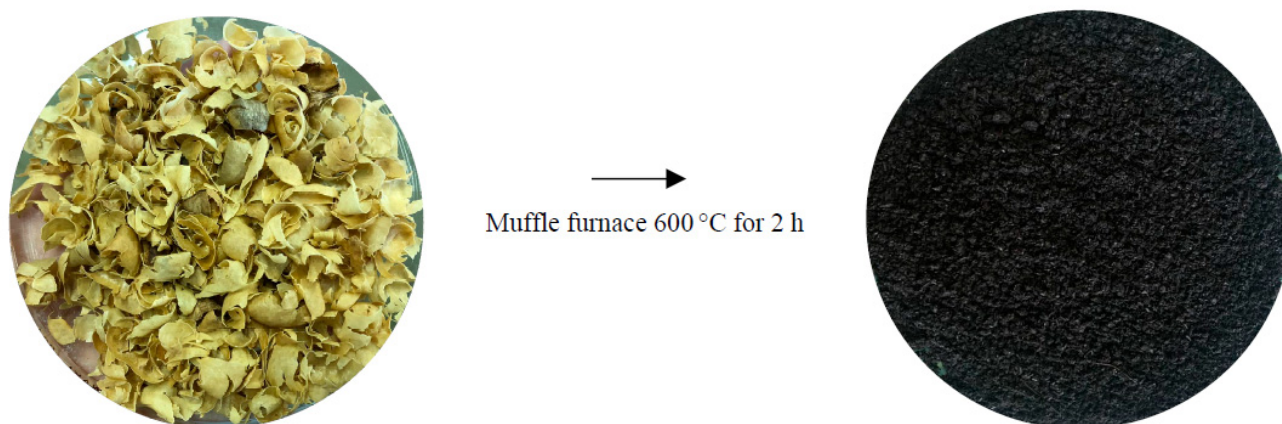


Figure 1. Morphological deformation of coffee husk into biochar.

2.4. Characterization of Adsorbent

The pH zero-point charge (pH_{zpc}) was also defined in this study for better understanding of the characteristics of this adsorbent. Samples were subjected to different initial pHs (2.0, 4.0, 6.0, 8.0, and 10.0) of NaCl (0.01 M). Mixture of NaCl (50 mL) with 0.1 g adsorbent was shaken for 24 h using a shaker before being centrifuged for 15 min at 1500 rpm. Then, the pH was measured for calculation of pH_{zpc} . Analysis of SEM images and functional groups CHB-Fe₃O₄ before and after adsorption were carried out by using SEM (JIED-2300, Shimadzu, Kyoto, Japan) and FTIR (Thermo Scientific Nicolet iS10, Waltham, MA, USA), respectively.

2.5. Detection of Glyphosate and Calibration Curve

The technique for detecting glyphosate was conducted by using the method discovered by [29]. The standard solution of 1000 mg/L glyphosate was used to prepare different concentrations of glyphosate (10, 20, 30, 40, and 50 mg/L). For detection of glyphosate, 0.5 mL of each standard glyphosate/sample were added into test tubes containing 0.5 mL of 5% (m/v) C₉H₆O₄ and 0.5 mL of 5% (m/v) Na₂MoO₄. The solution mixture was then heated in a water bath at a temperature ranging from 80 to 90 °C for 12 min until the sample solution turned a purple color. The sample was cooled down to room temperature, placed in a volumetric flask, and added 1 mL of distilled water. A spectrophotometer from Kyoritsu Chemical-Check (Lab., Corp, Yokohama, Japan) with a wavelength of 570 nm was used to measure the absorbance. From the measurement of the standard solution data, linear absorbance of the standard curve was obtained as the concentration of glyphosate increased, as presented in Figure 2.

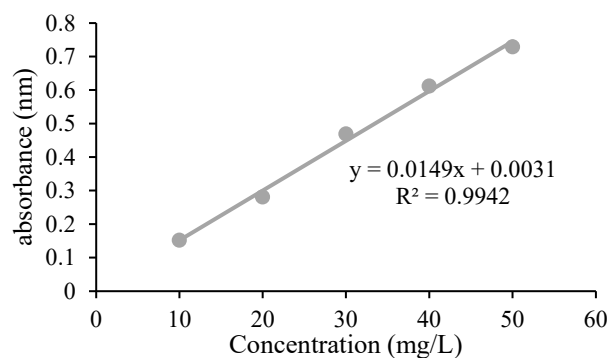


Figure 2. Standard curve of glyphosate, wavelength 570 nm.

2.6. Batch Adsorption and Desorption Experiments

CHB-Fe₃O₄ (0.05 g) was added into the 25 mL glyphosate solution and shaken at 30 °C with a bioshaker (V-BR-36). The influence of different experimental parameters (pH: 2.0, 4.0, 6.0, 8.0, and 10; initial glyphosate concentration: 10, 20, 30, 40, and 50 mg/L; contact time: 30, 60, 90, 150, 180, 240, 300, and 1440 min) were investigated. An external magnet was used to separate the adsorbent from the adsorbate. Quantification of adsorbed glyphosate was calculated using Equation (1), while Equation (2) was applied to determine the removal percentage. All procedures were conducted twice [30,31].

$$q_e = \frac{C_a - C_e}{W} \times V \quad (1)$$

$$\% \text{ removal} = \frac{C_a - C_e}{C_a} \times 100 \quad (2)$$

where C_a and C_e are the initial and after concentration of glyphosate (mg/L), respectively. q_e is the adsorption quantity (mg/g), W is the mass of adsorbent (g), and V is the glyphosate volume (L).

2.7. Desorption Studies

Desorption studies were performed using the equilibrium data. NaOH was used as the desorption solvent. Different concentrations of NaOH (0.1, 0.5, and 1 M), contact times (30–1440 min), and temperatures (30, 40, and 50 °C) were conducted to determine the effect of these parameters on desorption efficiency. The calculation for desorption percentage is presented in Equation (3) below [16].

$$\% \text{ desorption} = \frac{D_e}{A_e} \times 100 \quad (3)$$

where % desorption is the percent desorption (%), D_e and A_e are the desorption equilibrium and adsorption equilibrium (mg/g), respectively.

3. Results and Discussion

3.1. SEM Results of CHB-Fe₃O₄

Figure 3 shows SEM images of CHB-Fe₃O₄ before and after adsorption of glyphosate. It can be observed that the surface of CHB-Fe₃O₄ before adsorption is rougher and contains many available pores compared to the surface of the adsorbent after glyphosate adsorption. This could be due to the interactions between the adsorbate and adsorbent, where the adsorbate (glyphosate) diffuses into the available pores on the surface of the adsorbent (CHB-Fe₃O₄), and the binding of glyphosate to the active sites of the adsorbent containing Fe₃O₄. Based on the results of a study by [32], the porosity structure of magnetite coffee husk, obtained from SEM results, is in accordance with the BET results of coffee husk biochar and magnetic coffee husk biochar samples, which are 48.84 m²/g and 142.32 m²/g, respectively. This information signifies that the adsorption ability of magnetite coffee husk biochar is better than coffee husk biochar.

3.2. FTIR Spectra of Adsorbent before and after Glyphosate Adsorption

The FTIR data before and after the adsorption are shown in Figure 4. The band at 3369 cm⁻¹ changed to 3341 cm⁻¹ after adsorption, indicating a strong interaction between O-H surface groups and glyphosate [33,34]. The band at 2119 cm⁻¹ changed to 2117 cm⁻¹ after adsorption of glyphosate which was specific to the functional group of C≡C [35]. The peak band at 1630 cm⁻¹'s move to 1629 cm⁻¹ after adsorption is attributed to the C=O group [36]. The peak at the 1118 cm⁻¹ and 1124 cm⁻¹ bands demonstrates the (C-O) polysaccharide carbohydrate region [37]. In contrast, bands at 883 and 888 cm⁻¹ were assigned to C-H vibrations in the aromatic structures [36]. The bands at 632 cm⁻¹ and 598 cm⁻¹ are the result of the stretching vibrational interaction which connected to the

metal–oxygen bonds in the Fe–O bond of the Fe_3O_4 crystal lattice [38]. Based on previous research conducted by [32], comparison of FTIR results showed that the OH, C–H, and C=C functional groups in raw coffee husk become more obvious after turned into coffee husk biochar, because of hydrothermal carbonization process making the intensity of the FTIR spectrum of the coffee husk biochar become higher and more obvious. The thermal process causes the raw coffee husk to have more OH and C=C functional groups. Furthermore, the chemical treatment by adding magnetite (Fe_3O_4) into coffee husk biochar has resulted in more oxygen-containing functional groups in the adsorbent.

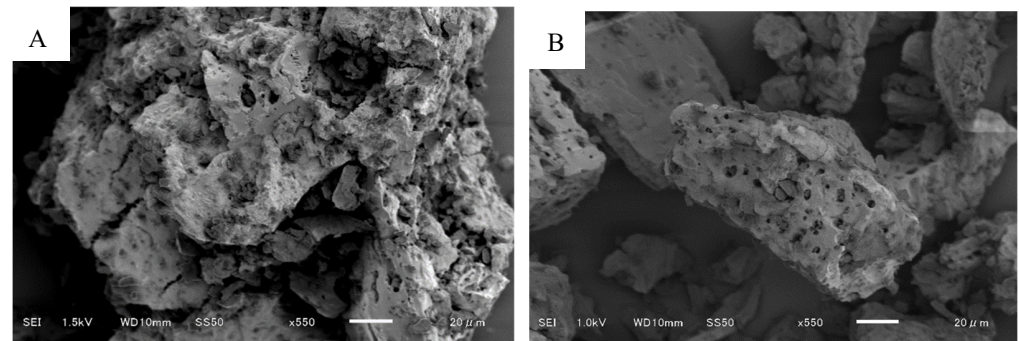


Figure 3. SEM of CHB- Fe_3O_4 before (A) and after (B) adsorption glyphosate.

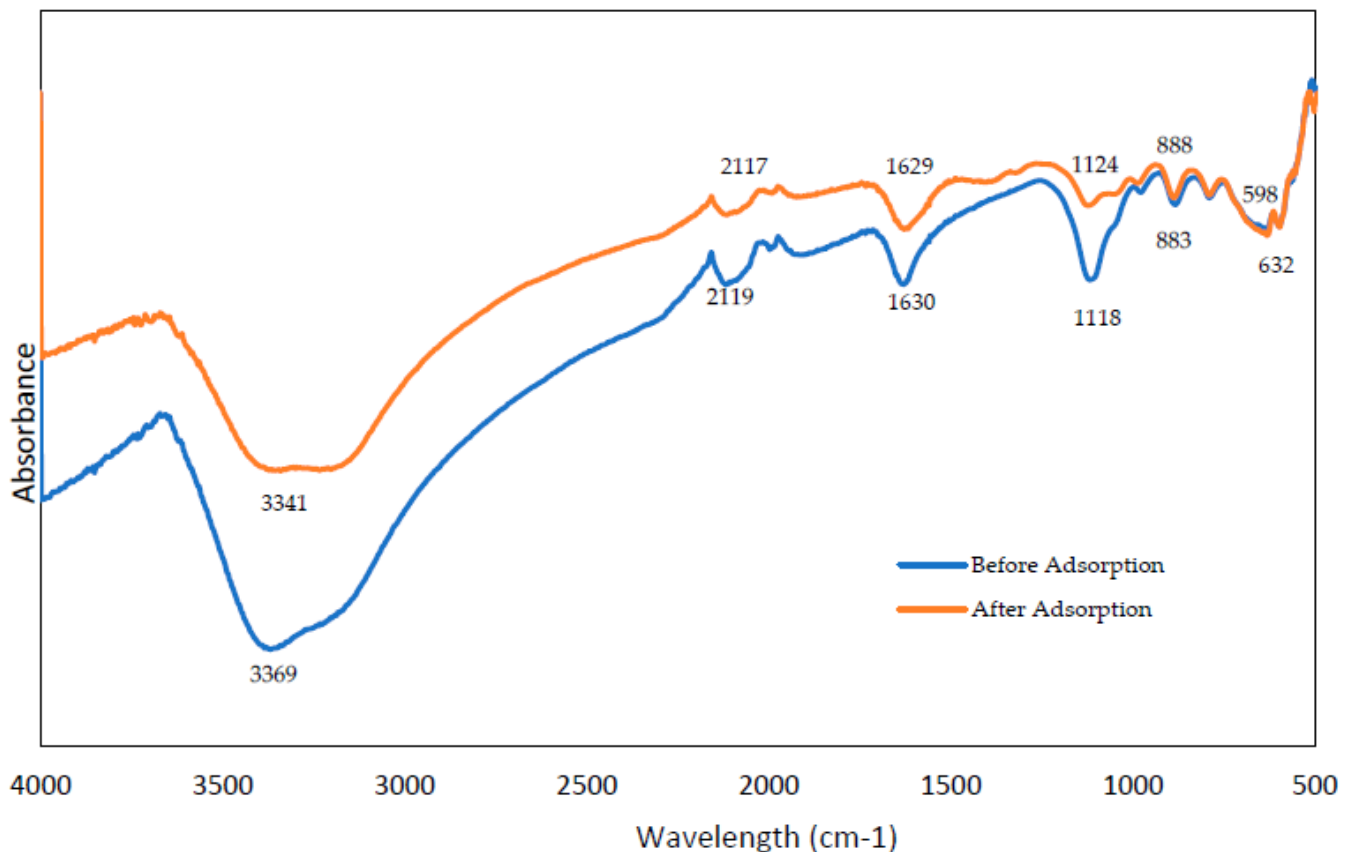


Figure 4. FTIR spectra of adsorbent before and after glyphosate adsorption.

3.3. Interaction Glyphosate with CHB- Fe_3O_4

After adsorption of glyphosate using CHB- Fe_3O_4 , it is assumed that there will be several interactions occurring between the adsorbent and the adsorbate as shown in Figure 5. Previous studies explained that there are several interactions defined in glyphosate adsorption such as pore diffusion, electrostatic interactions, and H-bonding [39,40]. Pore diffusion

is the interaction that is most likely to occur, because the glyphosate will move into the adsorbent through the available pore sites.

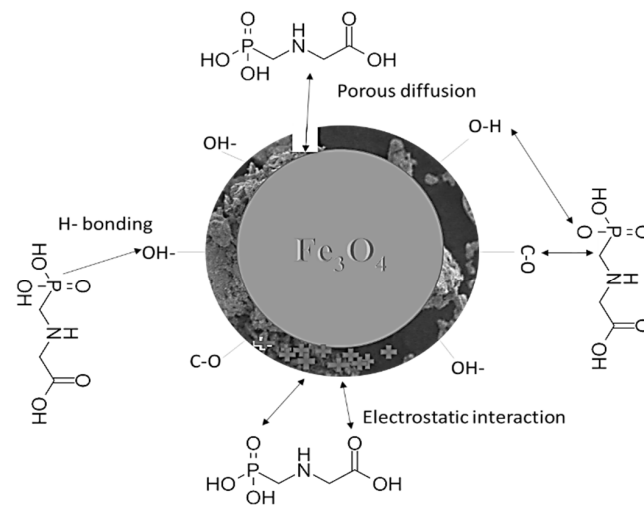


Figure 5. Proposed mechanism of glyphosate adsorption.

3.4. Initial pH Effects

The pH is one of the most important parameters that affect the surface charge of the adsorbate (glyphosate) and adsorbent (CHB-Fe₃O₄). As shown in Figure 6a the highest adsorption was obtained at pH 2, with an adsorption capacity of 3.07 mg/g after 30 min of adsorption. Figure 6b shows that the pH_{zpc} was at pH 2. If the $pH < pH_{zpc}$, the adsorbent surface will be positively charged, while if the $pH > pH_{zpc}$, the surface of the adsorbent will be negatively charged. At pH 2, the surface of the adsorbent is positively charged, while glyphosate is negatively charged because the pK_a of glyphosate is 2.23 (< 2.23 is negative charge). Thus, electrostatic interactions between the net charge of the adsorbent and the negative charge of glyphosate occurred. The lower pH caused the deprotonation of amine (NH⁻), phosphate (PO₃⁻), and carboxyl (COOH⁻) groups in glyphosate molecules [10,11,15,41].

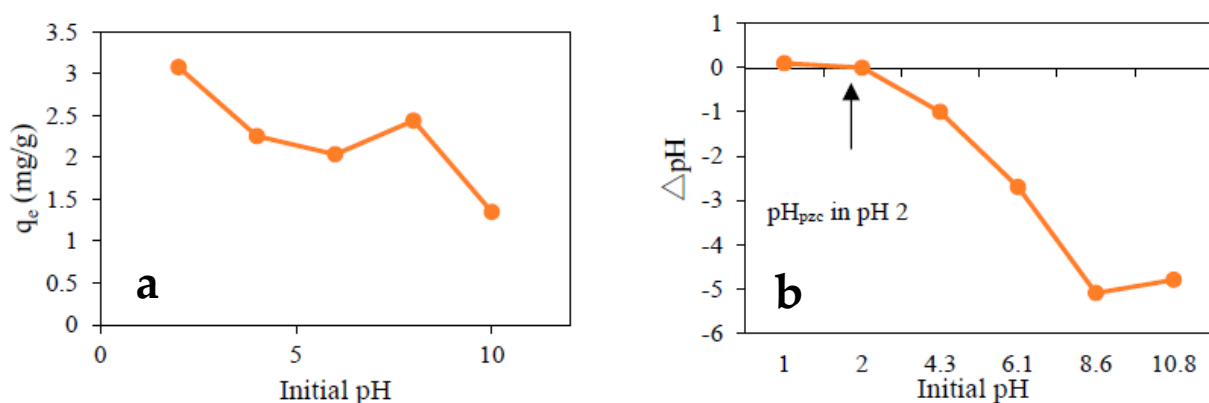


Figure 6. (a) Effects of initial pH of adsorption: CHB-Fe₃O₄ 0.05 g; initial glyphosate: 10 mg/L, volume (mL): 25; temperature: 30 °C; and time: 30 min (b) pH_{pzc} of CHB-Fe₃O₄.

3.5. Initial Concentration Effects

The effect of the initial concentration is shown in Figure 7. The result displays an increase in adsorption capacity from 2.77 to 17.13 mg/g when the glyphosate concentration increases. This is because the quantity of glyphosate molecules increases with increasing concentration, resulting in a greater tendency for attachment of the adsorbate onto the adsorbent surface [42].

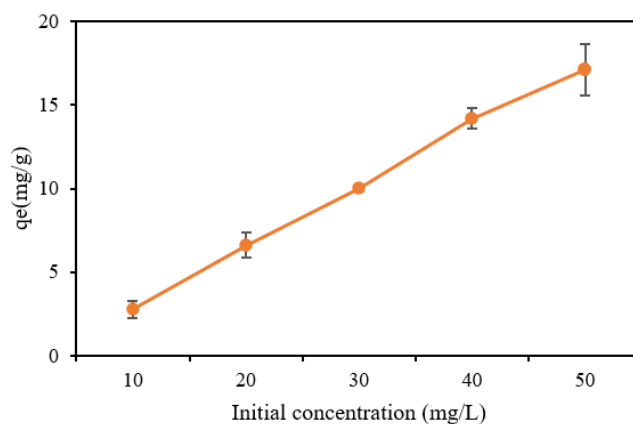


Figure 7. Effects of initial concentration of glyphosate adsorption: CHB-Fe₃O₄ 0.05 g; pH: 2; volume (mL): 25; temperature: 30 °C; and time: 30 min.

3.6. Adsorption Isotherm Studies

Isotherm models are a crucial concept for observing or predicting the processes that occur during adsorption equilibrium [43]. The Langmuir and Freundlich models are the most commonly used models for glyphosate adsorption and are used for isotherm analysis in this study. The Langmuir isotherm shows that active sites of the adsorbent have equal energy and that the adsorption process primarily occurs with regards to monolayers [39,40,44]. In contrast, the Freundlich isotherm shows that energy declines logarithmically as the number of molecules adsorbed on the adsorbent sites increases [7,9,40,45]. The experiment was conducted by adding 0.05 g of adsorbent into 25 mL of glyphosate at different initial concentrations ranging from 10 to 50 mg/L. The linear equations for the Langmuir and Freundlich models are listed in Table 1.

Table 1. Linear equations of isotherm models.

Model	Equation	Supporting Equation
Langmuir	$C_e/q_e = \frac{C_e}{q_{max}} + 1/(K_L q_{max})$	$R_L = \frac{1}{(1+K_L \times C_a)}$
Freundlich	$\ln q_e = \ln k_F + \frac{1}{n} \times \ln C_b$	

Note: q_e = adsorption capacity (mg/g), K_L = equilibrium constant of adsorption (L/mg), K_f = equilibrium constant of adsorption, q_{max} = maximal adsorption capacity (mg/g), C_e and C_a (mg/L) = equilibrium concentration and initial concentration, respectively.

q_{max} in the Langmuir equation indicates that the maximum adsorption capacity obtained in this study was 18.315. R_L is the separation factor, where $0 <$ (favorable), > 1 (unfavorable) and $= 1$ (linear). Table 2 shows that the R_L value of glyphosate adsorption was 0.0146, indicating that the adsorption was favorable [16]. The graph in Figure 8a shows that the regression coefficient R^2 in the Freundlich equation was close to one, making it more suitable than the Langmuir model (Figure 8b).

Table 2. Isotherm Constants for Glyphosate Adsorption.

Adsorption Isotherm	Isotherm Constant	Glyphosate
Langmuir	q_{max}	18.315
	K_L	0.6727
	R_L	0.0146
	R^2	0.2178
Freundlich	K_F	4.1783
	$1/n$	1.3711
	R^2	0.8456

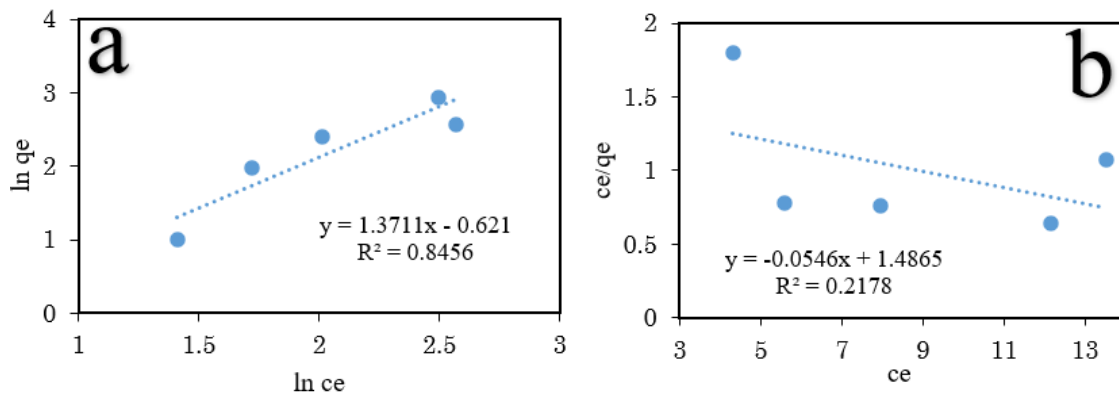


Figure 8. Linear curves of adsorption isotherm studies. (a): Freundlich, (b): Langmuir. (CHB-Fe₃O₄: 0.05 (g), volume: 25 (mL), pH: 2, time: 240 min, and temperature: 30 °C).

3.7. Adsorption Kinetic Studies

Figure 9 shows the effect of contact time on glyphosate adsorption. The adsorption capacity increased rapidly from 30 to 60 min, and then steadily increased to 240 min with an adsorption capacity of 22.29 mg/g, then decreased and increased again until 1440 min. This is because the adsorbent's surface site was saturated with adsorbate, and this condition could lead to adsorption or desorption of the glyphosate. Finally, adsorption capacity equilibrium was attained at 1440 min with an adsorption capacity of 22.44 mg/g.

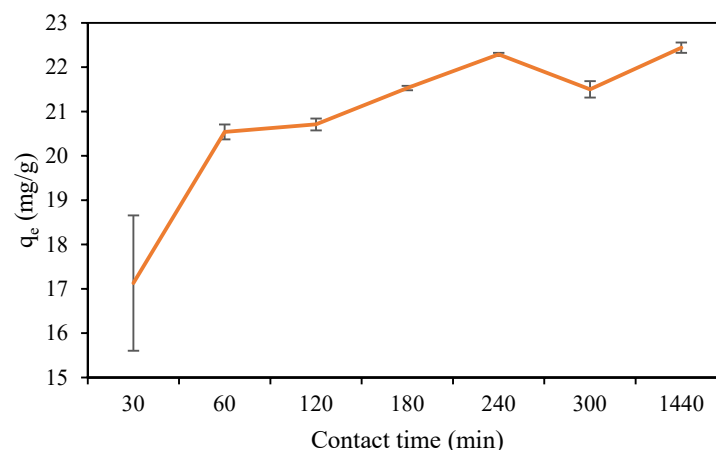


Figure 9. Effect of contact time on adsorption of glyphosate (CHB-Fe₃O₄: 0.05 (g), volume: 25(mL), glyphosate concentration 50 mg/L, and temperature: 30 °C).

Kinetic analysis can be helpful in determining the mechanism and pace of the adsorption process [18]. In this study, pseudo-first-order (Equation (4)) and pseudo-second-order (Equation (5)) models were used to predict the adsorption kinetic of this study.

$$\text{Log}(q_e - q_t) = \text{Log} q_e - k_1 t \quad (4)$$

$$t/q_t = (1/k_2 q_e^2) + t/q_e \quad (5)$$

where k_1 (min^{-1}) is the constant of the pseudo-first order, and k_2 (g/mg min^{-1}) is the constant of the pseudo-second order. t (time) (min), and q_t (mg/g) is the adsorption capacity at time.

The results show that the pseudo-second-order model ($R = 0.999$) (Figure 10) is more appropriate for describing the kinetic study data in this research, with an adsorption capacity of 22.57 mg/g (Table 3). These results are in line with those reported by a previous study [46], which showed that glyphosate adsorption using nanosized copper hydroxide-

modified resin fits the pseudo-second-order model, and chemisorption could be the rate-determining process.

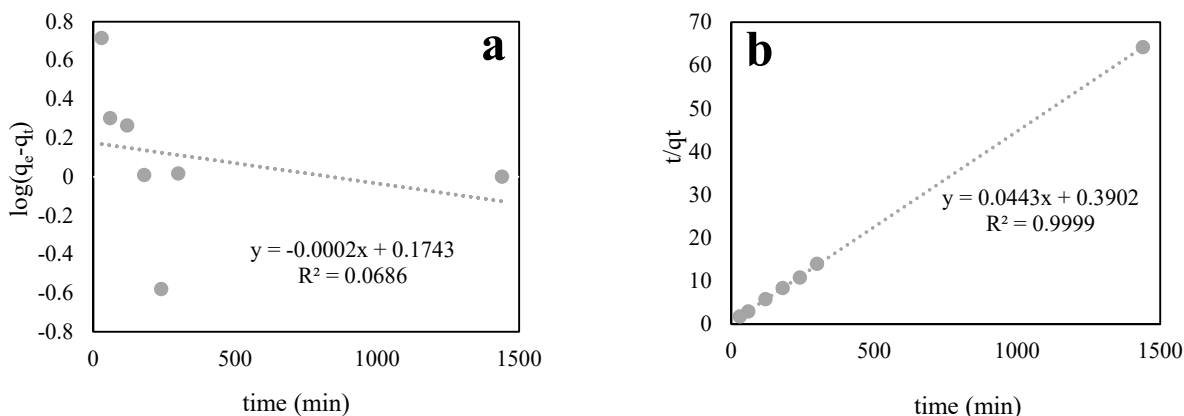


Figure 10. Linear curves of adsorption kinetic studies. (a): pseudo-first order, (b): pseudo-second order. CHB-Fe₃O₄: 0.05 (g); volume: 25 (mL); glyphosate concentration 50 mg/L; and temperature: 30 °C.

Table 3. Kinetic model parameters for adsorption of glyphosate with CHB-Fe₃O₄.

Pseudo-First-Order Model			Pseudo-Second-Order Model		
q _e (mg/g)	K ₁ (min ⁻¹)	R ²	q _e (mg/g)	K ₂ (g mg ⁻¹ min ⁻¹)	R ²
1.1904	1.38889 ⁻⁷	0.0686	22.5733	0.0050	0.9999

3.8. Desorption Study

The desorption percentages of glyphosate are shown in Figure 11. The results showed that the NaOH concentration significantly affects the release of glyphosate from the adsorbent. Increases in the concentrations of NaOH have the contrary effect on the desorption percentage, as the concentration of glyphosate released decreases from 69.40 to 5.99% (Figure 11a). Subsequently, different temperatures were also tested for desorption effectiveness, and the results showed that 30 °C is the best temperature for desorption of glyphosate (Figure 11b). Interestingly, the desorption of glyphosate varied as the time increased. The desorption percentage increased and then decreased for up to 1440 min, indicating the occurrence of adsorp/desorp during these processes (Figure 11c). The best results for desorption of glyphosate were obtained at a temperature of 30 °C by using NaOH (0.1 M) for 30 min, with a desorption percentage of 69.4%.

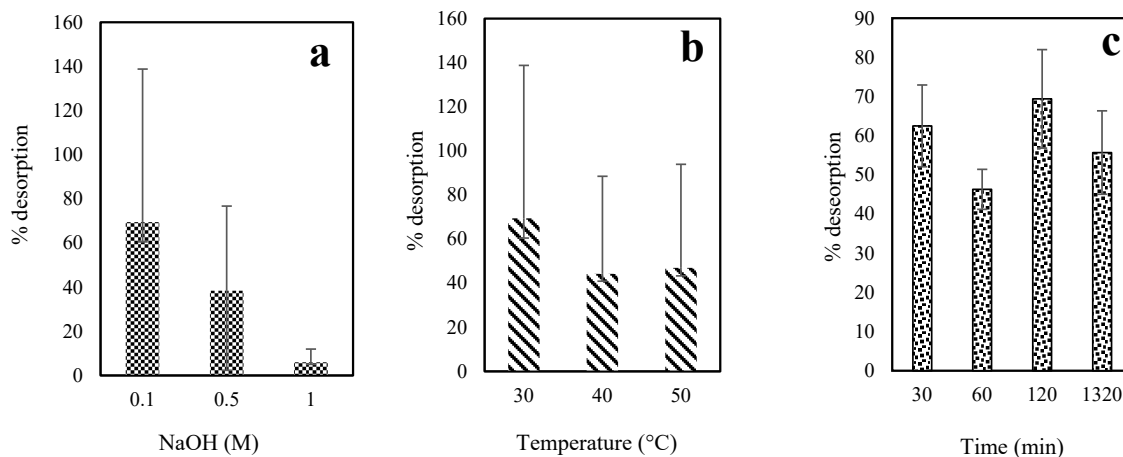


Figure 11. (a) Effect of initial concentration; (b) effect of initial temperature; (c) effect of initial time on glyphosate desorption.

Various materials have been reported in the literature for the adsorption-based removal of glyphosate, as shown in Table 4. The results indicate that CHB-Fe₃O₄ is a feasible adsorbent for the removal of glyphosate from water.

Table 4. Materials with capacity for adsorption of glyphosate reported in the literature.

Adsorbents	q _e (mg/g)	Reference
Woody Biochar	44	[9]
Zinc oxide nanoparticles	82.97	[21]
Synthesis of clay-biochar	37.06	[23]
Multi-walled carbon nanotubes (MWCNTs)	21.17	[47]
Cu-zeolite 4A	112.7	[48]
Nanosized Copper Hydroxide	140	[46]
CHB-Fe ₃ O ₄	22.44	This study

4. Conclusions

In this study, biochar-based coffee-husk-loaded Fe₃O₄ (CHB-Fe₃O₄) was used as an adsorbent to remove glyphosate from water. The results show that the best glyphosate adsorption was achieved at pH 2 solution after a contact time of 1440 min, with maximum adsorption capacity of 22.44 mg/g. The Freundlich model provided the best fit to the isotherm analysis, demonstrating multilayer sorption. The most effective model for characterizing the adsorption kinetics was the pseudo-second-order model, with chemical adsorption as the rate-limiting phase, possibly including valence forces by sharing or exchanging electrons between the adsorbent and the adsorbate. The desorption studies showed that the use of 0.1 M NaOH is the best concentration to achieve a desorption percentage of 69.4% in 30 min.

Author Contributions: Conceptualization, A.L.L.; methodology, A.L.L., E.H.; validation, E.H.; formal analysis, A.L.L., E.H., N.M.M.S.; investigation, A.L.L.; resources, H.H.; data curation, Y.M.; writing—original draft preparation, A.L.L., N.M.M.S.; writing—review and editing, A.L.L., E.H.; visualization, S.Y.; supervision, E.H., H., G., H.H.; project administration, H.H. All authors have read and agreed to the published version of the manuscript.

Funding: This research received no external funding.

Acknowledgments: The author (A.L.L.) would like to thank the Prefectural University of Hiroshima for providing an opportunity as a research exchange student in the Faculty of Bioresources Science and also thank to all authors to contribute for this article.

Conflicts of Interest: The authors declare no conflict of interest.

References

- Benbrook, C.M. Trends in glyphosate herbicide use in the United States and globally. *Environ. Sci. Eur.* **2016**, *28*, 3. [[CrossRef](#)]
- Hu, Y.S.; Zhao, Y.Q.; Sorohan, B. Removal of glyphosate from aqueous environment by adsorption using water industrial residual. *Desalination* **2011**, *271*, 150–156. [[CrossRef](#)]
- Myers, J.P.; Antoniou, M.N.; Blumberg, B.; Carroll, L.; Colborn, T.; Everett, L.G.; Hansen, M.; Landrigan, P.J.; Lanphear, B.P.; Mesnage, R.; et al. Concerns over use of glyphosate-based herbicides and risks associated with exposures: A consensus statement. *Environ. Health* **2016**, *15*, 19. [[CrossRef](#)]
- Meftaul, I.; Venkateswarlu, K.; Dharmarajan, R. Controversies over human health and ecological impacts of glyphosate: Is it to be banned in modern agriculture? *Environ. Pollut.* **2020**, *263*, 114372. [[CrossRef](#)]
- Ahmad, S.; Almeshadi, M.; Janjuhah, H.T.; Kontakiotis, G.; Abdulaziz, O.; Saeed, K.; Ahmad, H.; Allahyani, M.; Aljuaid, A.; Alsaiani, A.A.; et al. The Effect of Mineral Ions Present in Tap Water on Photodegradation of Organic Pollutants: Future Perspectives. *Water* **2023**, *15*, 175. [[CrossRef](#)]
- Fadaei, A.; Dehghani, M.; Mahvi, A.; Nasser, S.; Rastkari, N.; Shayeghi, M. Degradation of organophosphorus pesticides in water during UV/Htreatment: Role of sulphate and bicarbonate ions. *J. Chem.* **2012**, *9*, 2015–2022. [[CrossRef](#)]
- Herath, I.; Kumarathilaka, P.; Al-Wabel, M.I.; Abduljabbar, A.; Ahmad, M.; Usman, A.R.; Vithanage, M. Mechanistic modeling of glyphosate interaction with rice husk derived engineered biochar. *Microporous Mesoporous Mater.* **2016**, *225*, 280–288. [[CrossRef](#)]
- Jiang, Y.; Ni, D.; Ding, Q.; Chen, B.; Chen, X.; Kan, Y.; Dong, S. Synthesis and characterization of nano-crystalized HfC based on an aqueous solution-derived precursor. *RSC Adv.* **2018**, *8*, 39284–39290. [[CrossRef](#)] [[PubMed](#)]

9. Mayakaduwa, S.; Kumarathilaka, P.; Herath, I.; Ahmad, M.; Al-Wabel, M.; Ok, Y.S.; Usman, A.; Abduljabbar, A.; Vithanage, M. Equilibrium and kinetic mechanisms of woody biochar on aqueous glyphosate removal. *Chemosphere* **2016**, *144*, 2516–2521. [[CrossRef](#)] [[PubMed](#)]
10. Serra-Clusellas, A.; De Angelis, L.; Beltramo, M.; Bava, M.; De Frankenberger, J.; Vigliarolo, J.; Di Giovanni, N.; Stripeikis, J.D.; Rengifo-Herrera, J.A.; de Cortalezzi, M.M.F. Glyphosate and AMPA removal from water by solar induced processes using low Fe(III) or Fe(II) concentrations. *Environ. Sci. Water Res. Technol.* **2019**, *5*, 1932–1942. [[CrossRef](#)]
11. Valle, A.L.; Mello, F.C.C.; Alves-Balvedi, R.P.; Rodrigues, L.P.; Goulart, L.R. Glyphosate detection: Methods, needs and challenges. *Environ. Chem. Lett.* **2019**, *17*, 291–317. [[CrossRef](#)]
12. Song, J.; Li, X.-M.; Figoli, A.; Huang, H.; Pan, C.; He, T.; Jiang, B. Composite hollow fiber nanofiltration membranes for recovery of glyphosate from saline wastewater. *Water Res.* **2013**, *47*, 2065–2074. [[CrossRef](#)] [[PubMed](#)]
13. Zheng, T.; Sun, Y.; Lin, Y.; Wang, N.; Wang, P. Study on preparation of microwave absorbing MnOx/Al₂O₃ adsorbent and degradation of adsorbed glyphosate in MW–UV system. *Chem. Eng. J.* **2016**, *298*, 68–74. [[CrossRef](#)]
14. Yang, Y.; Deng, Q.; Yan, W.; Jing, C.; Zhang, Y. Comparative study of glyphosate removal on goethite and magnetite: Adsorption and photo-degradation. *Chem. Eng. J.* **2018**, *352*, 581–589. [[CrossRef](#)]
15. Nourouzi, M.M.; Chuah, T.G.; Choong, T.S.Y.; Rabiei, F. Modeling biodegradation and kinetics of glyphosate by artificial neural network. *J. Environ. Sci. Health-Part B Pestic. Food Contam. Agric. Wastes* **2012**, *47*, 455–465. [[CrossRef](#)]
16. Hidayat, E.; Yoshino, T.; Yonemura, S.; Mitoma, Y.; Harada, H. A Carbonized Zeolite/Chitosan Composite as an Adsorbent for Copper (II) and Chromium (VI) Removal from Water. *Materials* **2023**, *16*, 2532. [[CrossRef](#)]
17. Hidayat, S.E.; Khaekhum, S.; Yonemura, Y.M.; Harada, H. Biosorption of Eriochrome Black T Using *Exserohilum rostratum* NMS1.5 Mycelia Biomass. *J* **2022**, *5*, 427–434. [[CrossRef](#)]
18. Hidayat, E.; Yoshino, T.; Yonemura, S.; Mitoma, Y.; Harada, H. Synthesis, Adsorption Isotherm and Kinetic Study of Alkaline-Treated Zeolite/Chitosan/Fe³⁺ Composites for Nitrate Removal from Aqueous Solution—Anion and Dye Effects. *Gels* **2022**, *8*, 782. [[CrossRef](#)] [[PubMed](#)]
19. Ye, S.; Zeng, G.; Wu, H.; Zhang, C.; Liang, J.; Dai, J.; Liu, Z.; Xiong, W.; Wan, J.; Xu, P.; et al. Co-occurrence and interactions of pollutants, and their impacts on soil remediation—A review. *Crit. Rev. Environ. Sci. Technol.* **2017**, *47*, 1528–1553. [[CrossRef](#)]
20. Soares, D.; Silva, L.; Duarte, S.; Pena, A.; Pereira, A. Glyphosate use, toxicity and occurrence in food. *Foods* **2021**, *10*, 2785. [[CrossRef](#)]
21. Odoemelam, S.A.; Oji, E.O.; Okon, N.; Rajni, E. Zinc oxide nanoparticles adsorb emerging pollutants (glyphosate pesticide) from aqueous solutions. *Environ. Monit. Assess.* **2023**, *195*, 1–19. [[CrossRef](#)]
22. Hottes, E.; da Silva, C.O.; Bauerfeldt, G.F.; Castro, R.N.; de Lima, J.H.C.; Camargo, L.P.; Dall’antonia, L.H.; Herbst, M.H. Efficient removal of glyphosate from aqueous solutions by adsorption on Mg–Al-layered double oxides: Thermodynamic, kinetic, and mechanistic investigation. *Environ. Sci. Pollut. Res.* **2022**, *29*, 83698–83710. [[CrossRef](#)]
23. Rallet, D.; Paltaha, A.; Tsamo, C.; Loura, B. Synthesis of clay-biochar composite for glyphosate removal from aqueous solution. *Heliyon* **2022**, *8*, e09112. [[CrossRef](#)]
24. Junior, E.G.S.; Perez, V.H.; de Paula, S.C.S.E.; Silveira, T.d.C.; Olivares, F.L.; Justo, O.R. Coffee Husks Valorization for Levoglucosan Production and Other Pyrolytic Products through Thermochemical Conversion by Fast Pyrolysis. *Energies* **2023**, *16*, 2835. [[CrossRef](#)]
25. Oosterkamp, W.J. *Use of Volatile Solids from Biomass for Energy Production*; Elsevier: Amsterdam, The Netherlands, 2014. [[CrossRef](#)]
26. Hidayat, E.; Halem, H.I.A.; Mitoma, Y.; Harada, H. Recovery of Biomass Incinerated as Struvite-K Precipitates Followed Aluminium Removal. *Green Sustain. Chem.* **2021**, *11*, 96–106. [[CrossRef](#)]
27. Ayalew, A.A.; Aragaw, T.A. Utilization of treated coffee husk as low-cost bio-sorbent for adsorption of methylene blue. *Adsorpt. Sci. Technol.* **2020**, *38*, 205–222. [[CrossRef](#)]
28. Quyen, V.T.; Pham, T.H.; Kim, J.; Thanh, D.M.; Thang, P.Q.; Van Le, Q.; Jung, S.H.; Kim, T. Biosorbent derived from coffee husk for efficient removal of toxic heavy metals from wastewater. *Chemosphere* **2021**, *284*, 131312. [[CrossRef](#)] [[PubMed](#)]
29. Nagaraja, P.; Bhaskara, B.L. Sensitive spectrophotometric assessment of carbofuran using dapson as a new chromogenic reagent in formulations and environmental samples. *Eclética Química* **2006**, *31*, 43–48. [[CrossRef](#)]
30. Harada, H.; Hidayat, E.; Uemoto, S.; Fujita, K. Extraction of phosphorous from thermally treated sludge and separation of aluminum by adsorption. *J. Mater. Cycles Waste Manag.* **2021**, *23*, 2112–2119. [[CrossRef](#)]
31. Hidayat, E.; Harada, H.; Mitoma, Y.; Yonemura, S.; Halem, H.I.A. Rapid Removal of Acid Red 88 by Zeolite/Chitosan Hydrogel in Aqueous Solution. *Polymers* **2022**, *14*, 893. [[CrossRef](#)]
32. Hien, T.T.; Vu, N.T.; Thien, P.H.; Thanh, N.D.; Tuan, P.D. Synthesis of Novel Magnetic Adsorbents from Coffee Husks By Hydrothermal Carbonization. *Vietnam. J. Sci. Technol.* **2017**, *55*, 526–533. [[CrossRef](#)]
33. Keiluweit, M.; Nico, P.S.; Johnson, M.G. Dynamic Molecular Structure of Plant Biomass-Derived Black Carbon (Biochar). *Environ. Sci. Technol.* **2010**, *44*, 1247–1253. [[CrossRef](#)]
34. Kloss, S.; Zehetner, F.; Dellantonio, A.; Hamid, R.; Ottner, F.; Liedtke, V.; Schwanninger, M.; Gerzabek, M.H.; Soja, G. Characterization of Slow Pyrolysis Biochars: Effects of Feedstocks and Pyrolysis Temperature on Biochar Properties. *J. Environ. Qual.* **2012**, *41*, 990–1000. [[CrossRef](#)]
35. Xie, J.; Lin, R.; Liang, Z.; Zhao, Z.; Yang, C.; Cui, F. Effect of cations on the enhanced adsorption of cationic dye in Fe₃O₄-loaded biochar and mechanism. *J. Environ. Chem. Eng.* **2021**, *9*, 105744. [[CrossRef](#)]

36. Li, Y.; Tsend, N.; Li, T.; Liu, H.; Yang, R.; Gai, X.; Wang, H.; Shan, S. Microwave assisted hydrothermal preparation of rice straw hydrochars for adsorption of organics and heavy metals. *Bioresour. Technol.* **2019**, *273*, 136–143. [[CrossRef](#)] [[PubMed](#)]
37. Filley, T.R.; McCormick, M.K.; Crow, S.E.; Szlavecz, K.; Whigham, D.F.; Johnston, C.T.; Heuvel, R.N.v.D. Comparison of the chemical alteration trajectory of *Liriodendron tulipifera* L. leaf litter among forests with different earthworm abundance. *J. Geophys. Res. Biogeosciences* **2008**, *113*, G01027. [[CrossRef](#)]
38. Nalbandian, M.J.; Zhang, M.; Sanchez, J.; Nam, J.; Cwiertny, D.M.; Myung, N.V. Mesoporous θ -Alumina/Hematite (θ -Al₂O₃/Fe₂O₃) composite nanofibers for heavy metal removal. *Sci. Adv. Mater.* **2017**, *9*, 22–29. [[CrossRef](#)]
39. Samuel, L.; Wang, R.; Dubois, G.; Allen, R.; Wojtecki, R.; La, Y.H. Amine-functionalized, multi-arm star polymers: A novel platform for removing glyphosate from aqueous media. *Chemosphere* **2017**, *169*, 437–442. [[CrossRef](#)]
40. Herath, G.A.D.; Poh, L.S.; Ng, W.J. Statistical optimization of glyphosate adsorption by biochar and activated carbon with response surface methodology. *Chemosphere* **2019**, *227*, 533–540. [[CrossRef](#)]
41. Hosseini, N.; Toosi, M.R. Removal of 2,4-D, glyphosate, trifluralin, and butachlor herbicides from water by polysulfone membranes mixed by graphene oxide/TiO₂ nanocomposite: Study of filtration and batch adsorption. *J. Environ. Health Sci. Eng.* **2019**, *17*, 247–258. [[CrossRef](#)] [[PubMed](#)]
42. Moussavi, G.; Barikbin, B. Biosorption of chromium(VI) from industrial wastewater onto pistachio hull waste biomass. *Chem. Eng. J.* **2010**, *162*, 893–900. [[CrossRef](#)]
43. Sen, K.; Mondal, N.K.; Chattoraj, S.; Datta, J.K. Statistical optimization study of adsorption parameters for the removal of glyphosate on forest soil using the response surface methodology. *Environ. Earth Sci.* **2017**, *76*, 22. [[CrossRef](#)]
44. Jiang, X.; Ouyang, Z.; Zhang, Z.; Yang, C.; Li, X.; Dang, Z.; Wu, P. Mechanism of glyphosate removal by biochar supported nano-zero-valent iron in aqueous solutions. *Colloids Surfaces A Physicochem. Eng. Asp.* **2018**, *547*, 64–72. [[CrossRef](#)]
45. Nourouzi, M.M.; Chuah, T.G.; Choong, T.S.Y. Adsorption of glyphosate onto activated carbon derived from waste newspaper. *Desalin. Water Treat.* **2010**, *24*, 321–326. [[CrossRef](#)]
46. Zhou, C.; Jia, D.; Liu, M.; Liu, X.; Li, C. Removal of Glyphosate from Aqueous Solution Using Nanosized Copper Hydroxide Modified Resin: Equilibrium Isotherms and Kinetics. *J. Chem. Eng. Data* **2017**, *62*, 3585–3592. [[CrossRef](#)]
47. Diel, J.C.; Franco, D.S.; Igansi, A.V.; Cadaval, T.R.; Pereira, H.A.; Nunes, I.d.S.; Basso, C.W.; Alves, M.D.C.M.; Morais, J.; Pinto, D.; et al. Green synthesis of carbon nanotubes impregnated with metallic nanoparticles: Characterization and application in glyphosate adsorption. *Chemosphere* **2021**, *283*, 131193. [[CrossRef](#)]
48. Zavareh, S.; Farrokhzad, Z.; Darvishi, F. Modification of zeolite 4A for use as an adsorbent for glyphosate and as an antibacterial agent for water. *Ecotoxicol. Environ. Saf.* **2018**, *155*, 1–8. [[CrossRef](#)]

Disclaimer/Publisher’s Note: The statements, opinions and data contained in all publications are solely those of the individual author(s) and contributor(s) and not of MDPI and/or the editor(s). MDPI and/or the editor(s) disclaim responsibility for any injury to people or property resulting from any ideas, methods, instructions or products referred to in the content.